Accepted Manuscript

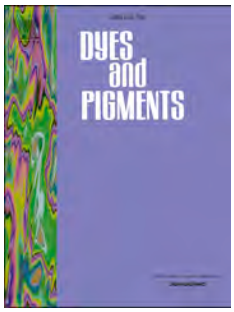

Modification of the electronic properties of the π-spacer of chromophores linked to calix[4]arene platform for DSSCs applications

E. Colom, J.M. Andrés-Castán, D. Barrios, I. Duerto, S. Franco, J. Garín, J. Orduna, B. Villacampa, M.J. Blesa

PII: S0143-7208(18)31199-9

DOI: https://doi.org/10.1016/j.dyepig.2018.12.066

Reference: DYPI 7271

To appear in: *Dyes and Pigments*

Received Date: 29 May 2018

Revised Date: 30 December 2018

Accepted Date: 30 December 2018

Please cite this article as: Colom E, Andrés-Castán JM, Barrios D, Duerto I, Franco S, Garín J, Orduna J, Villacampa B, Blesa MJ, Modification of the electronic properties of the π-spacer of chromophores linked to calix[4]arene platform for DSSCs applications, *Dyes and Pigments* (2019), doi: https://doi.org/10.1016/j.dyepig.2018.12.066.

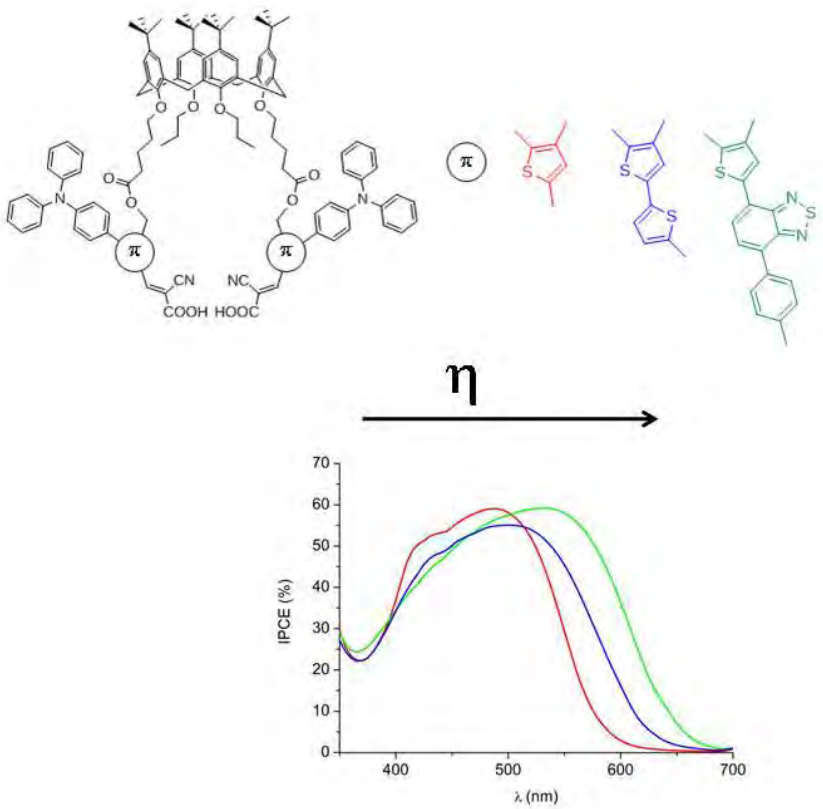

Modification of the electronic properties of the π-spacer of chromophores linked to calix[4]arene platform for DSSCs applications

E. Colom [a], J. M. Andrés-Castán [a], D. Barrios [b], I. Duerto [a], S. Franco [a], J. Garín [a], J. Orduna [a], B. Villacampa [b], M. J. Blesa [a,*]

Address:
[a] Departamento de Química Orgánica, ICMA
Universidad de Zaragoza-CSIC
50009, Zaragoza (Spain)
Phone: (+34) 876 553507
E-mail: mjblesa@unizar.es

[b] Departamento de Física de la Materia Condensada, ICMA
Universidad de Zaragoza-CSIC
50009, Zaragoza (Spain)

Corresponding author:

Dr. María-Jesús Blesa: mjblesa@unizar.es

Authors:

Eduardo Colom: ecolomsienes@gmail.com

José María Andrés-Castán: jmandrescastan@gmail.com

Daniel Barrios: 790772@unizar.es

Isolda Duerto: isolda@unizar.es

Dr. Santiago Franco: sfranco@unizar.es

Prof. Javier Garín: jgarin@unizar.es

Dr. Jesús Orduna: jorduna@unizar.es

Dr. Belén Villacampa: bvillaca@unizar.es

Dr. María-Jesús Blesa: mjblesa@unizar.es

Modification of the electronic properties of the π-spacer of chromophores linked to calix[4]arene platform for DSSCs applications

E. Colom [a], J. M. Andrés-Castán [a], D. Barrios [b], I. Duerto [a], S. Franco [a], J. Garín [a], J. Orduna [a], B. Villacampa [b], M. J. Blesa [a] *

Abstract

We have developed two novel dyes based on *p-tert*-butyl-calix[4]arene in order to evaluate their behavior as sensitizer in photovoltaic devices. These dyes consist in a difunctionalized calix[4]arene with triphenylamine (TPA)-donor, a heteroaromatic π-conjugated spacer, thiophene and benzothiadiazole-phenyl ring, respectively and cyanoacetic acid as acceptor group. The effect of the π-spacer has been studied by UV-vis spectroscopy and Differential Pulse Voltammetry and the models compounds have been theoretically investigated. The dye bearing phenylbenzothiadiazole results in a bathochromic shifted absorption and an adequate efficiency to transfer charge from D to A. The considerable increase of the photocurrent density results in a better efficiency of the devices prepared with these novel dyes with respect to the *p-tert*-butyl-calix[4]arene derivatives bearing TPA dye. In particular, *p-tert*-butyl-calix[4]arene derivative based on phenylbenzothiadiazole has reached an efficiency value of 5.84 % which means an increase of 33 % of the efficiency over those calix[4]arene derivatives with TPA dye.

Keywords
metal-free sensitizer, multichromophore, calix[4]arene, aggregation, benzothiadiazole.

Introduction

Solar energy, as a source of renewable energy, has several advantages with respect to traditional energy sources as it is inexhaustible; it is accessible from any geographical location and has reduced environmental impacts. From early 90's, organic dyes have received attention with respect to their application in dye sensitized solar cells (DSSCs). [1] A great variety of Donor-π-spacer-Acceptor (D–π–A) dyes for sensitized solar cells have been studied due to their facile synthetic process, flexibility and efficiency. [2] The D–π–A structure leads to photoinduced intramolecular charge transfer from the donor to the acceptor unit, which is effective to favor the electron transfer between the dye and the TiO_2 semiconductor.

Increasing the light harvesting ability of the DSSCs is of great importance to obtain better overall power conversion efficiency. This can be achieved through increasing the molar extinction coefficient of the sensitizer, broadening the absorption region and increasing the dye loading on TiO_2 films. [3] Recently, it was found that a double D–π–A branched organic dye, with a non-conjugated alkyl linkage to connect two separate D–π–A fragments, leads to a larger adsorption amount of the D–π–A segment on the TiO_2 film compared to the single D–π–A dye. Thus the cells based on double D–π–A branched dye may exhibit higher short-circuit current density (J_{sc}), open-circuit voltage (V_{oc}) and photoconversion efficiency (η). [4]

One disadvantage of organic sensitizers in DSSCs is the aggregate formation, which leads to instability of the excited state, and reduces electron injection. [5,6] Aggregation can be avoided either by using different co-adsorbents or by introducing bulky groups in the dye [7,

8,9]. In this way, charge recombination processes are prevented and the stability of the system is improved. [10-11]

Therefore, we designed new dyes based on a *p-tert*-butyl-calix[4]arene scaffold to be used as DSSC sensitizers because of the versatility of the calix[4]arene, which can be readily functionalized. [12,13] Our research group has used the *p-tert*-butyl-calix[4]arene scaffold to integrate several chromophores in one single molecule, far away enough to behave as independent chromophores and so providing several light-harvesting units per molecule which favors high molar extinction coefficients. [14-16] Moreover, the *p-tert*-butyl substituted calix[4]arene derivative has bulky alkyl chains. This functionalization increases the solubility of the systems and hinders dye aggregation. In addition, these systems can be immobilized in cone conformation by the introducing of propyl or longer groups into the lower rim. [17,18] Despite of the fact that calix[4]arene derivatives possess so many applications, [19,20] the investigation of calix[4]arene-based sensitizers as a key component in DSSCs has been scarcely studied. The role of calix[4]arene as donor unit was reported by Tan *et al.* [21] and two papers have been published by our research group using the *p-tert*-butyl-calix[4]arene as scaffold to orient the anchoring groups. [15,16] In our previous work [15], it was shown that the molar extinction coefficient of the two branched dye with TPA increased when it is compared with the monosubstituted calix[4]arene. However, the IPCE spectrum showed that the injection of photons above 600 nm is negligible. In the present work, the expansion of the absorption spectrum is intended, via the variation of the π-spacer. The nature of the π-spacer is relevant in order to tune the photophysical properties. [22] Joly *et al.* published interesting results based on a thiophene and a benzothiadiazole-phenyl heterocycle as π-spacer. [23] The use of thiophene-based π–bridge provides chemical stability to the final dye. Moreover, the use of a dissymmetric π–conjugated bridge (A'–π) including a benzothiadiazole (BTZ) [23,24], an electro deficient unit (A') localized close to the triphenylamine-thiophene part and a phenyl ring between the (A') unit and the anchoring cyanoacrylic acid group stabilizes the dye radical cation and decreases the recombination rate. [25] To explore the impact of the electron-withdrawing ability of the auxiliary acceptor (A') and understand the effect of BTZ, we systematically investigated the photophysical, electrochemical and photovoltaic properties of the novel dyes. The pursuit of an efficient light harvester, as well as the inhibition of both the intermolecular π–π aggregation and the recombination processes can lead to an effective molecular design of sensitizers and to establish a relationship between the dye structure and the photovoltaic properties of these new branched dyes.

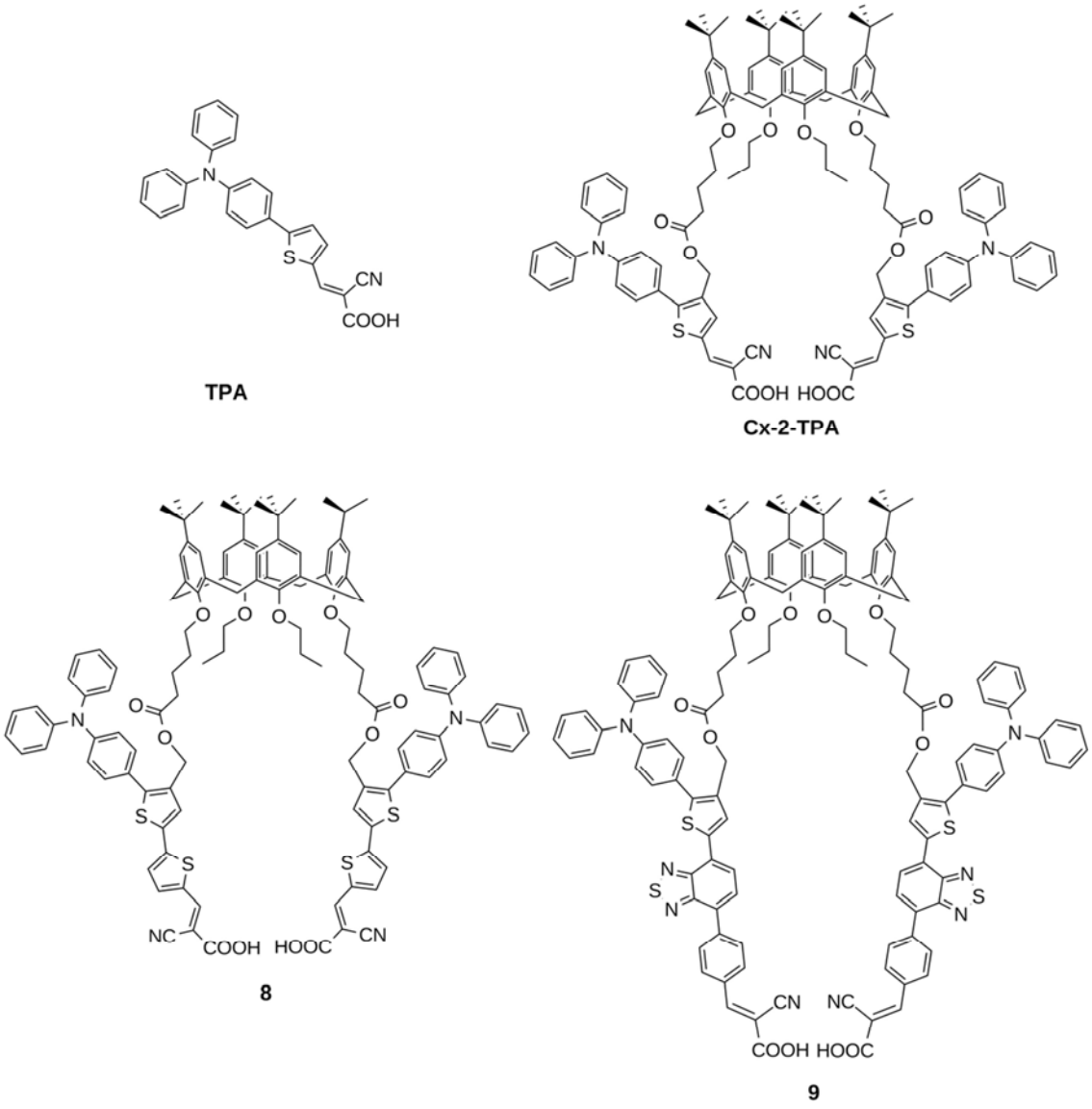

Chart 1. Structures of dyes **TPA**, **Cx-2-TPA**, **8** and **9.**

2.1 Synthesis and characterization

Chart 1 shows the molecular structure of **Cx-2-TPA**, **8** and **9**. **Cx-2-TPA** [15] is a calix[4]arene derivative of TPA dye [26] that it is used in this paper to compare its photovoltaic properties with those of compounds **8** and **9**.

Scheme 1 depicts the synthesis of compounds **4** and **5**. The TPA-thiophene derivative **1** was lithiated with *n*-BuLi in the 5 position and substituted with tributyltin chloride. [27] Then, the intermediate stannane STN was not stable and it was used in the next step without previous purification. The reactions of the donor moiety with the corresponding π-spacers (the commercial 5-bromo-2-thiophenecarboxaldehyde and 4-bromo-7-(4-formylphenyl)-2,1,3-benzothiadiazole) [28,29] were carried out by the Stille cross coupling reaction with $Pd(PPh_3)_4$, which is a versatile carbon-carbon bond formation reaction [30] and therefore aldehydes **2** and **3** were prepared. Finally, the *tert*-butyldimethylsilyl group of compounds **2** and **3** was removed with tetrabutylammonium fluoride (TBAF) in anhydrous tetrahydrofuran (THF) at room temperature to give the desired alcohol derivatives **4** and **5**.

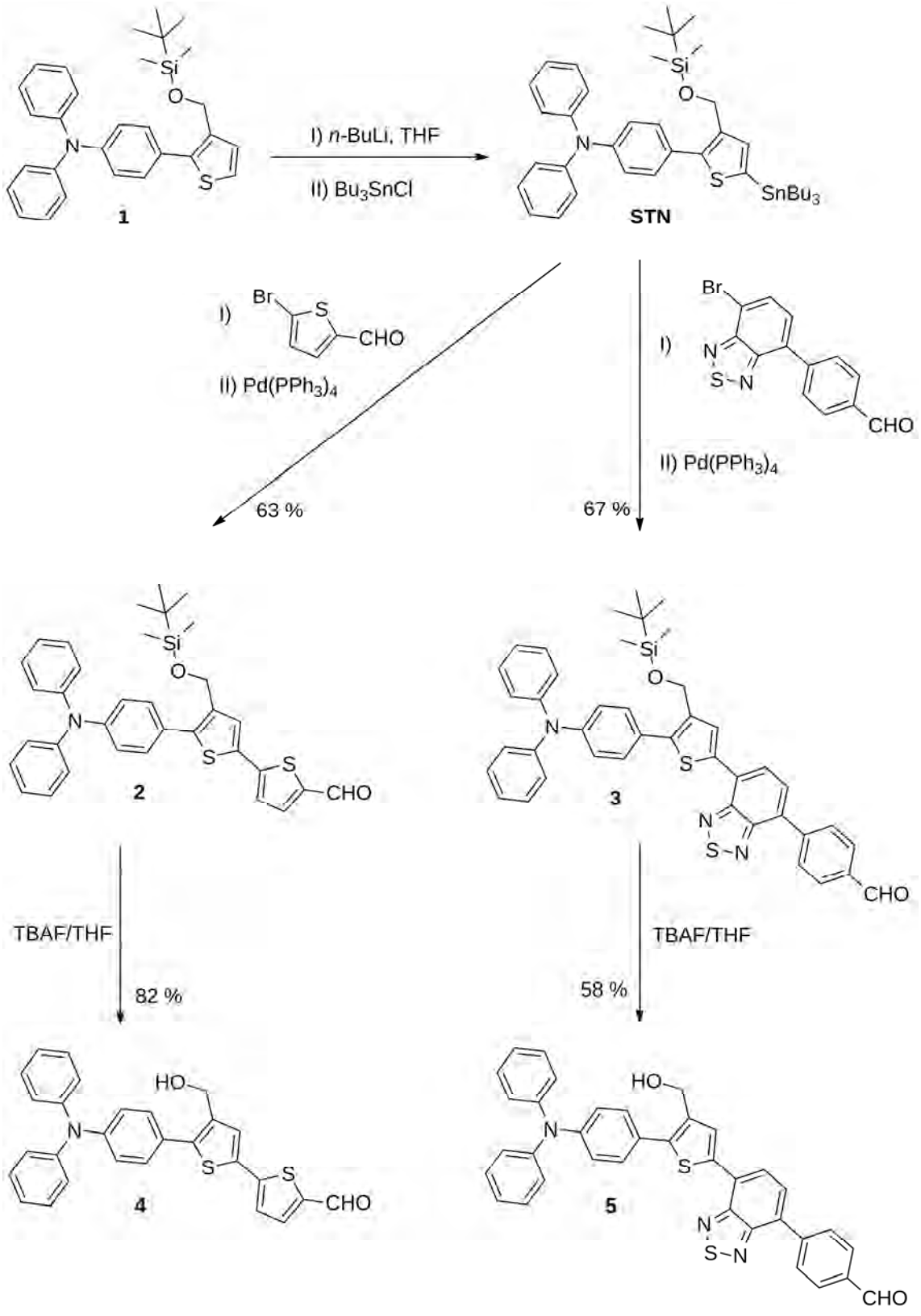

Scheme 1. Synthesis of the compounds **4** and **5.**

Aldehydes **6** and **7** were prepared by a Steglich reaction of the hydroxyl group of compounds **4** and **5**, using 1-ethyl-3-(3-dimethylaminopropyl)carbodiimide (EDC), with the corresponding carboxylic acid derivative of calixarene **Cx-2**, following the method described in the literature.

[31-33] (The detailed synthesis procedure is reported in Supporting Information). In the last synthetic step, the acceptor unit was incorporated by a Knoevenagel condensation of the formyl group with cyanoacetic acid in basic media and the dianchored dyes **8** and **9** were obtained (**Scheme 2**).

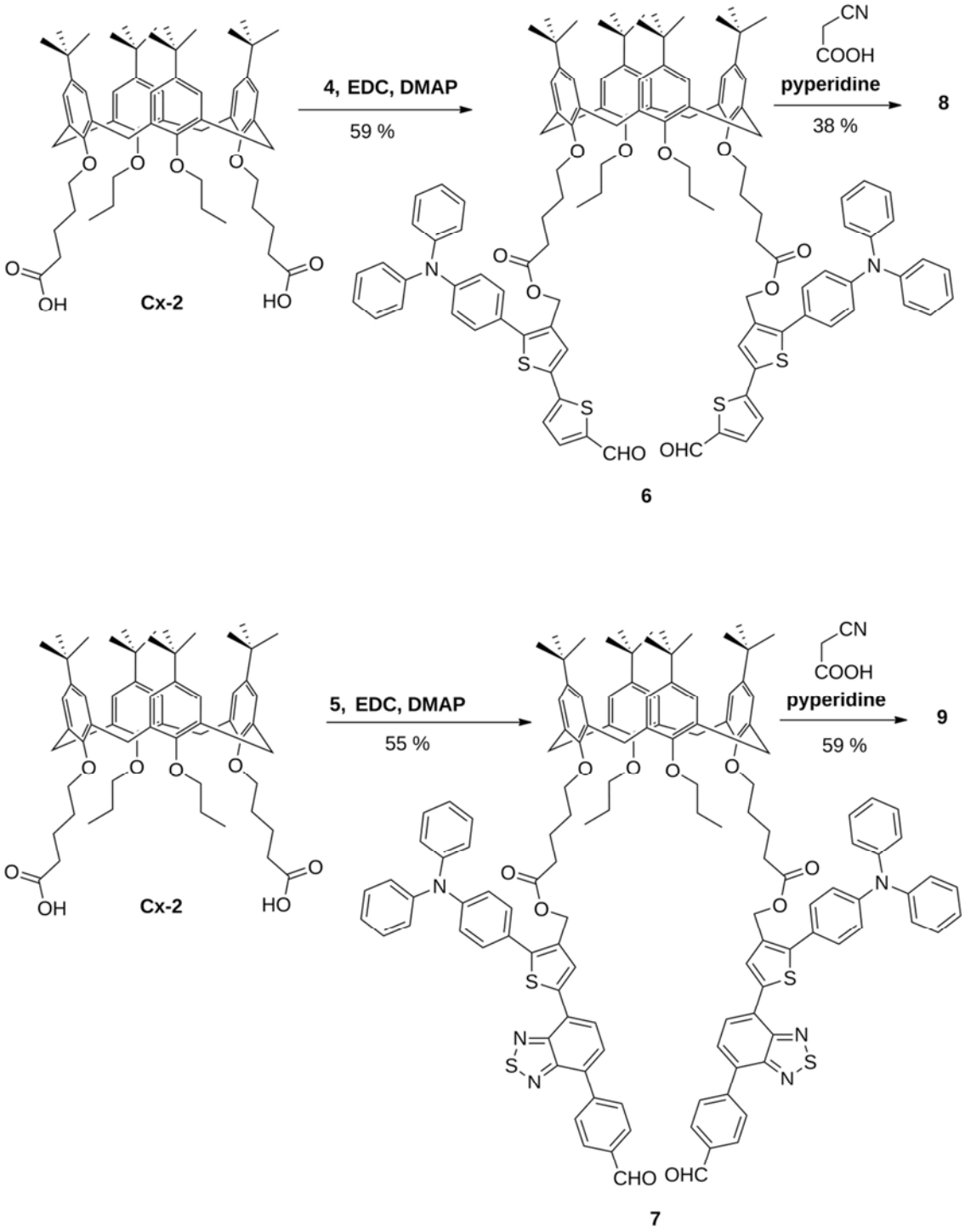

Scheme 2. Synthesis of the dyes **8** and **9.**

2.2. Optical properties

The UV-vis absorption measurements have been carried out in solutions (10^{-5} M THF, (**Fig. 1**)) and on sensitized TiO_2 films (**Fig. 2**). The spectrum of **9** shows a higher energy band centered at 340 nm, which is attributed to $\pi \rightarrow \pi^*$ electronic transition from the conjugated chain (BTZ). The spectral range at lower energy shows a band in the visible region (400-575 nm), which can be assigned to the intramolecular charge transfer (ICT) that occurs between the electron-withdrawing and electron-donating parts of both dyes **8** and **9**, respectively. [23,34] **8** and **9** present both broad bands up to ~ 600 nm. Taking into account this broad absorption, quite high short-circuit photocurrent density (J_{sc}) can be expected. [35]

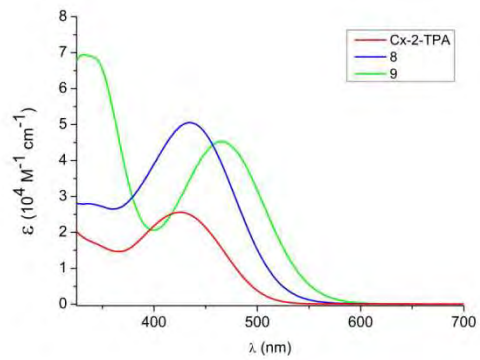

Fig. 1. Absorption spectra of **Cx-2-TPA**, **8** and **9** in THF solution (10^{-5} M).

Table 1 summarizes the optical properties of **Cx-2-TPA**, **8** and **9**. The molar extinction coefficient of the new dyes increases with respect to **Cx-2-TPA** [15] and also with respect to other triphenylamine-based dyes. [26,35,36] The new dyes exhibit high molar extinction coefficient values, indicating that these sensitizers have good light-absorption ability (Supporting Information, Fig. S.3 - S.5).

Table 1. Optical parameters of dyes **Cx-2-TPA**, **8** and **9.**

Dye	λ_{abs} [a] (nm)	λ_{abs} [b] (nm)	ε · [a] (10^4 M^{-1}·cm^{-1})
Cx-2-TPA	425	416	2.58 ± 0.16
8	436	424	5.03 ± 0.34
9	464	467	4.53 ± 0.46

[a] In THF solution (10^{-5} M). [b] Absorption on TiO_2 films.

Concerning the comparison of ICT bands shown in **Fig.1**, it should be noted that the lengthening of the spacer in dyes **8** and **9**, incorporating heterocycles, with respect to **Cx-2-TPA** results in a bathochromic shift and an increased molar extinction coefficient which points to a potential higher light –harvesting efficiency. Moreover, as it was expected, dye **9** with a benzothiadiazole unit shows bathochromic shifted absorption as compared with dye **8**.

Absorption bands for **8** and **9** shift to lower energies (by 14 and 8 nm, respectively) when tetrahydrofurane is changed by dichloromethane as solvent (Supporting Information, Fig. S.6). This phenomenon may be attributed to the interaction of polar solvent molecules with the carboxylic acid, which decreases the electron withdrawing strength of the acceptor by coordinating with COOH group.

The UV spectra of the films prepared with the studied dyes adsorbed on TiO_2 are shown in **Fig.2** and **Fig.S.7** (Supporting Information). When **8** and **Cx-2-TPA** are attached to the TiO_2 surface, the absorption maxima are slightly blue shifted when compared to those in THF solution. In general, the blue shifts can be ascribed to the deprotonation of the dyes and/or the formation of *H*-aggregates (extended head to tail stacking) [37] on the TiO_2 surface. It should be mentioned that the UV-vis spectra of the films of **Cx-2-TPA, 8** and **9** taken after different time intervals of immersion (5 and 24 h) do not show evidence of aggregation. The broad absorption bands of **8** and **9** on TiO_2 are adequate for effective light absorption.

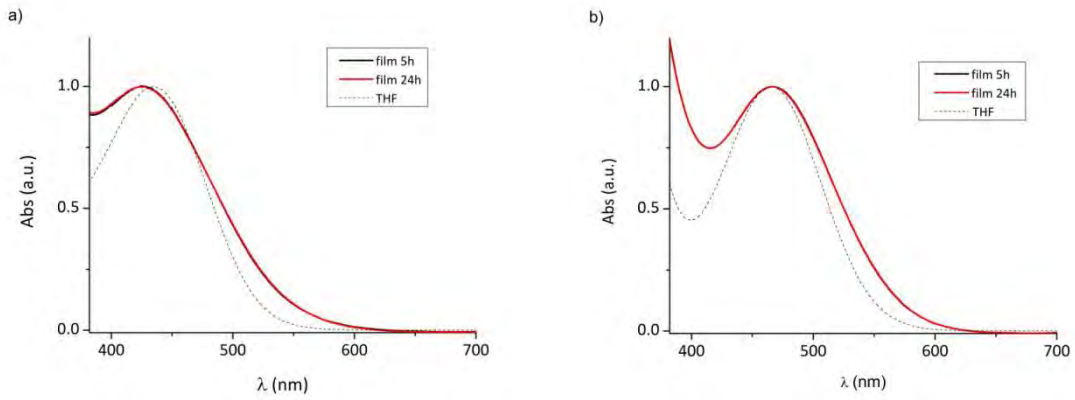

Fig. 2. UV-vis spectra of films (——) prepared with dyes a) **8** and b) **9** after 5 and 24 h of immersion. The spectra of THF solution (with maxima also normalized to unity) (-----) are shown for comparison.

2.3. Electrochemical properties

The electrochemical properties of **Cx-2-TPA**, **8** and **9** were studied by Differential Pulse Voltammetry (DPV). The voltammograms were performed using 0.1 M tetrabutylammonium hexafluorophosphate as supporting electrolyte, a glassy carbon working electrode, a Pt counter electrode and the Ag/AgCl reference electrode. The concentration of dye solutions was $5 \cdot 10^{-4}$ M in THF. The voltammograms are reported in the Supporting Information (**Figures S.10** and **S.12**). The oxidation potential of both ground and excited states of these dyes are gathered in **Table 2**.

Table 2. Transition energy $E_{0\text{-}0}$ and potential values E_{ox} and E_{ox}^*

Dye	E_{ox} [a] (V)	$E_{0\text{-}0}$ [b] (eV)	E_{ox}^* [c] (V)
Cx-2-TPA	+1.38	2.45	–1.06
8	+1.34	2.38	–1.04
9	+1.33	2.25	–0.92

[a] The oxidation potential values were converted to normal electrode (NHE) by addition of 0.199 V. [b] $E_{0\text{-}0}$ was estimated from the absorption spectra. [c] The estimated oxidation potential of excited state of the dye was calculated from $E^*_{ox} = E_{ox} - E_{0\text{-}0}$.

In the context of DSSCs, sensitizer dyes must satisfy several electrochemical requirements. On the one hand, the oxidation potential of the ground state of the dye, E_{ox} value, must be more positive than the redox potential of the electrolyte (in our case I_3^-/I^-, which has a value of +0.4 V [38]) to ensure that the dye is effectively regenerated after being oxidized. On the other hand, the oxidation potential of the excited state of the dye, E_{ox}^* value, must be more negative

than the TiO_2 conduction band (– 0.5 V vs NHE [39]) to favor the electron injection from the excited dye onto the TiO_2 electrode. [40,41] Dyes **Cx-2-TPA**, **8** and **9** have similar values of E_{ox} because the triphenylamine fragment is common. The values of E_{ox}^* varies depending on the π-spacer used. Due to the stronger accepting character, the E_{ox}^* potential for **9** is more positively shifted compared to **8** (≈ 0.12 V). The oxidation potential values of **Cx-2-TPA**, **8** and **9** (E_{ox} and E_{ox}^*) suggest that electron injection and regeneration are energetically permitted. (Supporting Information, Fig. S.13).

2.4. Theoretical calculations

In order to obtain further information on the electronic structure of the new dyes we have performed DFT calculations using acetyl derivatives **Ac-8** and **Ac-9** (**Chart 2**) as simplified models of calixarene derivatives **8** and **9**. The results of the calculations have been also compared to the acetyl derivative **Ac-TPA** [16] used as a simpler analogous of compound **Cx-2-TPA**.

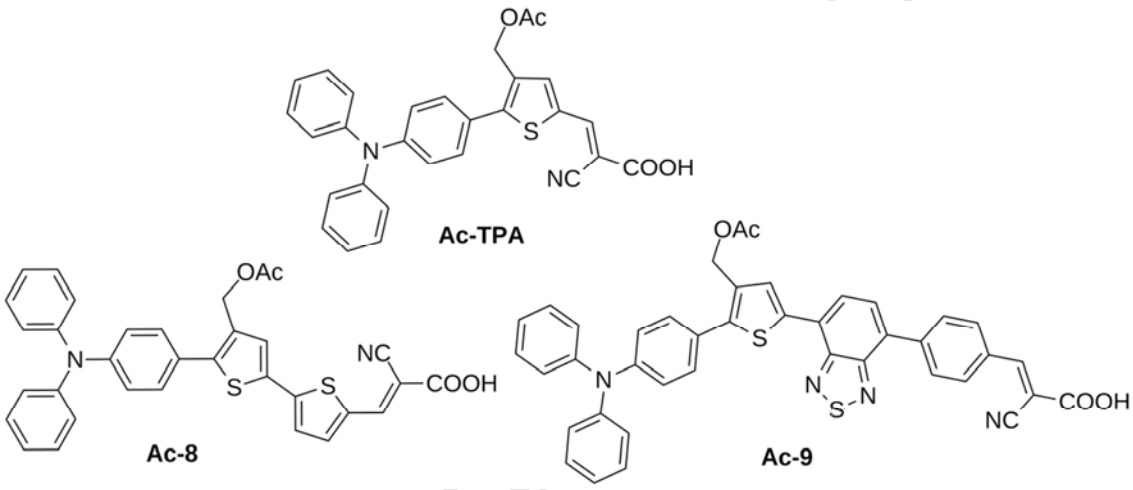

Chart 2. Molecular models used in theoretical calculations.

The optimization of ground state geometries reveals a twisted geometry along the π-conjugated spacer. The torsion angle between the phenylene and thiophene ring is 39-40º in the three studied dyes. The substitution of a thiophene ring in **Ac-8** by a benzothiazole-phenyl in **Ac-9** leads to an increased torsion, thus, the torsion between the two thiophene rings in acetyl derivative **Ac-8** is 12º and the geometry of **Ac-9** is even more twisted since the dihedral angle between thiophene and benzothiadiazole is 17º and between benzothiadiazole and the phenylene ring 37º. The optimized geometry of the first excited state of these dyes leads to a more planar geometry. This behavior was also observed in analogous triphenylamine derived dyes. [16] The Cartesian coordinates of all the calculated molecular geometries are included as supplementary material.

The most relevant calculated parameters are gathered in **Table 3.**

Table 3. Calculated[a] parameters of compounds **Ac-TPA**, **Ac-8** and **Ac-9.**

Dye	E_{HOMO} (eV)	E_{LUMO} (eV)	λ^b (nm)	f	E_{ox}^c (V)	$E_{0\text{-}0}$ (eV)	$E^*_{ox}{}^{c,d}$ (V)
Ac-TPA	-6.62	-2.15	425	1.15	+1.33	2.52	–1.19
Ac-8	-6.53	-2.30	451	1.55	+1.26	2.34	–1.08
Ac-9	-6.48	-2.42	453	1.42	+1.22	2.27	–1.04

[a] Calculated using the M06-2x/6-311+G(2d,p) model chemistry and the CPCM solvation model in THF. [b] Equilibrium CPCM values. [c] Referenced to Normal Hydrogen Electrode (NHE). [d] The oxidation potential of excited state of the dye was calculated from $E^*_{ox} = E_{ox} - E_{0\text{-}0}$. *f:* oscillator strength

The calculated values (**Table 3**) are in a good agreement with the experimental ones (**Tables 1** and **2**). The linkage of new heterocyclic rings in the π-spacer leads to slightly destabilized HOMO and stabilized LUMO energies, compared to **Ac-TPA**. This produces a slightly higher E^*_{ox} and lower E_{ox}, HOMO-LUMO gaps and $E_{0\text{-}0}$.

The lowest energy absorption is HOMO to LUMO in character with the HOMO mainly located on the donor side and the LUMO on the acceptor side of the dyes (**Fig. 3**). The extension of the conjugated spacer moving from **Ac-TPA** to **Ac-8** or **Ac-9** leads to increased oscillator strength values *(f)* accounting for higher light harvesting efficiencies.

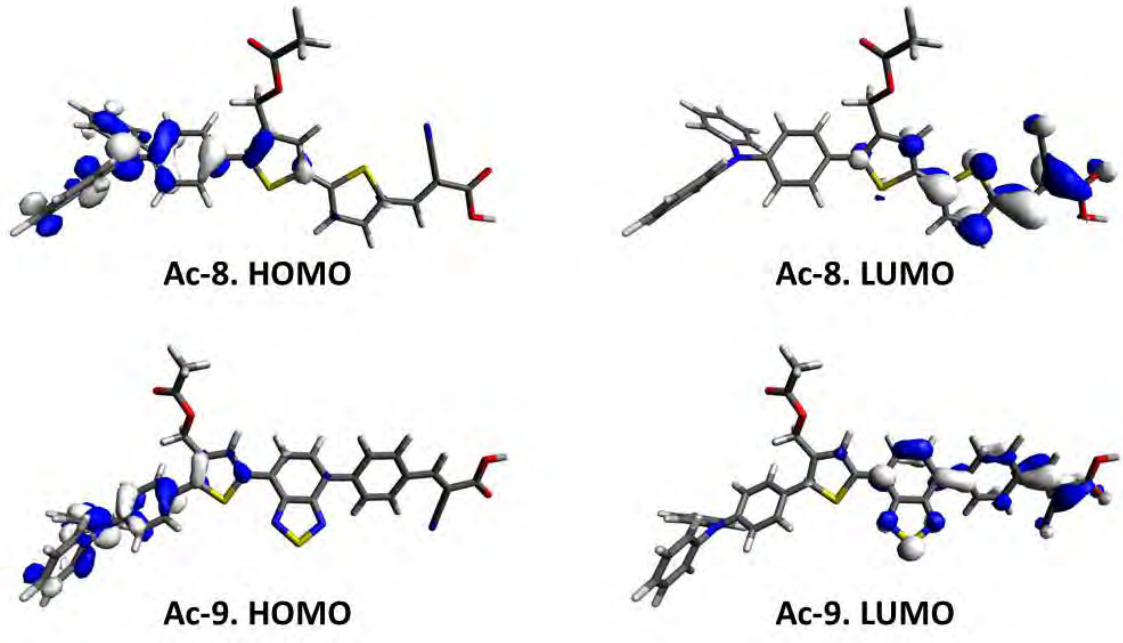

Fig. 3. Contour plots of frontier orbitals (0.04 isosurface value).

The calculation of the spin density of oxidized **Ac-8** and **Ac-9** (**Fig. 4**) reveals that the electron has been mainly extracted from the HOMO and therefore the electron hole locates on the donor side of the dyes. The molecular torsion prevents the extension of spin density to the acceptor side linked to the TiO_2. As reported by Roh *et al.* this fact avoids the undesirable back electron transfer (BET). [42]

a) b)

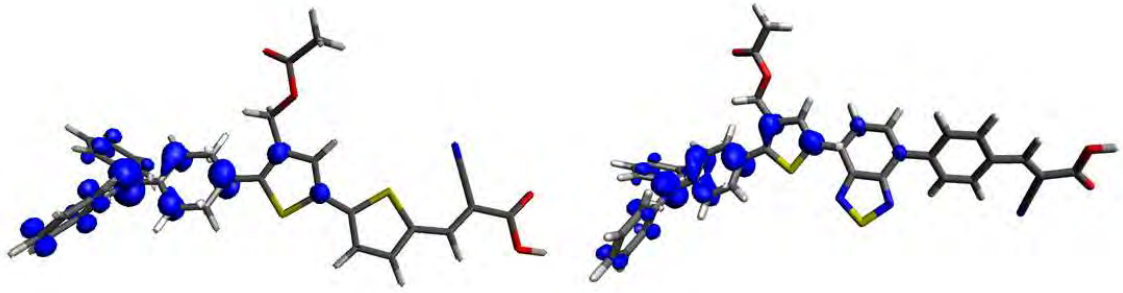

Fig. 4. Contour plots of the spin density of radical cations derived from a) **Ac-8** and b) **Ac-9** (0.004 isosurface value).

2.5. Photovoltaic Properties

The photovoltaic properties of the DSSC prepared with the sensitizers were studied. Based on previous studies, the starting conditions for the preparation of the devices were defined as 0.1 mM DCM solutions for dyes and an electrolyte based on the classical I_3^-/I^- system (1-butyl-3-methylimidazolium iodide (0.53 M), LiI (0.10 M), I_2 (0.050 M) and *tert*-butylpyridine (0.52 M) in anhydrous acetonitrile).

Fistly, devices were prepared with **Cx-2-TPA, 8** and **9** using 6 µm thick anodes and 5 h as immersion time (see Supporting Information for details). The results obtained upon their photovoltaic characterization are depicted in **Fig. 5** and **Table 4**.

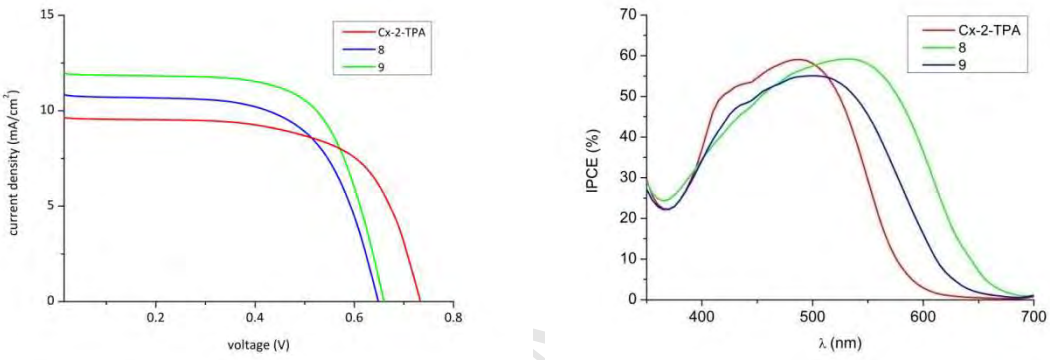

Fig. 5. a) Photocurrent density vs Photovoltage (left) under AM 1.5 G simulated solar light (100 mW cm^{-2}); b) Incident photon to converted electron efficiency (IPCE) spectra for DSSCs (6 µm thick electrodes) based on studied dyes (immersion time 5 h).

Devices prepared with new calix[4]arene derivative **9** exhibited better efficiencies than those prepared with **8** and **Cx-2-TPA**. **Fig 5** (right) depicts the IPCE spectra, broader for the devices with derivatives **8** and **9** than for **Cx-2-TPA** based on DSSCs. In particular, the device prepared with dye **9** showed the broadest IPCE spectrum (**Fig. 5** right). These devices are active up to 650 nm, region in which the electrons are yet quite efficiently collected. According to that the J_{sc} value of these cells prepared with **9** is higher than those prepared with **8** and **Cx-2-TPA** dyes. Regarding the voltage, the V_{oc} value is also slightly higher for **9** than for **8** based on DSSCs (**Table 4**).

Table 4. Average value of the measured photovoltaic parameters: open circuit voltaje (Voc), short circuit current density (Jsc), fill factor (ff) and overall efficiency (η). Three cells of each type were prepared and characterized (Experimental conditions: 6 µm thick electrodes of Dyesol 18NR-AO (paste). 0.1 mM DCM dye solution, 5 h immersion).

Dye	Dye loading mol/cm^2	J_{sc} (mA/cm^2)	V_{oc} (V)	*ff* (%)	η (%)
Cx-2-TPA	6.1 10^{-8}	9.86	0.74	63	4.59
8	5.1 10^{-8}	10.84	0.65	63	4.39
9	4.2 10^{-8}	11.95	0.66	66	5.19

The higher J_{sc} values of dye **9**-based devices agree with the theoretical results discussed in section 2.4. The theoretical calculations showed that the additional phenylene ring (inserted between **BTZ** unit and the anchoring group in **9**) is twisted with respect to the π -conjugated donor and **BTZ** part. In addition, they revealed that upon formation of the radical cation of **9**, the out-of-plane torsion of the adjacent **BTZ** and cyanoacrylic acid unit leads to an interruption of the π –conjugation between donor and anchoring groups that, according to Roh et al. [42], inhibits the back electron transfer which would be a good solution to improve the J_{SC} value.

Concerning the amount of dye adsorbed on TiO_2 film, the highest value (6.1 10^{-8} mol/cm^2) has been reached by **Cx-2-TPA** whereas the dye loading is sensibly higher for **8** (5.1 10^{-8} mol/cm^2) than for **9** (4.2 10^{-8} mol/cm^2). Despite the lowest amount in the latter, the better photovoltaic performance of **9**-chromophore-devices points to a promising molecular structure of this calixarene derivative with benzothiadiazole.

Looking for optimized conditions, devices using 6 µm thick electrodes and 24 h as immersion time were prepared. In spite of the longer immersion time, similar efficiency values were obtained for the three dyes. Finally, thicker electrodes where checked. The results of the photovoltaic characterization of the devices prepared with 13 µm thick electrodes and 24 h as immersion time are shown in **Fig. 6** and **Table 5**.

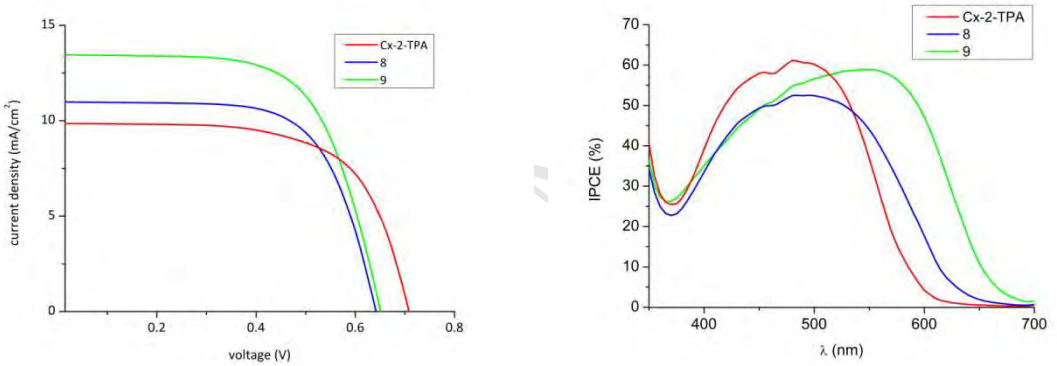

Fig. 6. a) Photocurrent density vs Photovoltage (left) under AM 1.5 G simulated solar light (100 mW cm-2); b) Incident photon to converted electron efficiency (IPCE) spectra (right) for DSSCs (13 µm thick electrodes) based on studied dyes (immersion time 24 h).

Table 5. Average value of the measured photovoltaic parameters: open circuit voltaje (V_{oc}), short circuit current density (J_{sc}), fill factor (*ff*) and overall efficiency (η). Three cells of each type were prepared and characterized (Experimental conditions: 13 µm thick electrodes of Dyesol 18NR-AO (paste). 0.1 mM DCM dye solution, 24 h immersion).

Dye	Dye loading mol/cm^2	J_{sc} (mA/cm^2)	V_{oc} (V)	*ff* (%)	η (%)
Cx-2-TPA	1.3 10^{-7}	9.51	0.70	66	4.40
8	1.3 10^{-7}	10.98	0.64	67	4.70
9	1.0 10^{-7}	13.52	0.66	66	5.84

Comparing **Table 4** and **5**, it can be observed that, when thicker electrodes are used, higher (up to 13 %) efficiencies were obtained for dye **9**, especially due to an improvement of the J_{sc} values. The decrease observed on V_{oc} value, actually very low in the case of **8** and **9,** can be attributed to an increase of the recombination processes when thicker electrodes are used.

Electrochemical impedance spectroscopy (EIS) is a very useful tool to study the electron transport kinetics in DSSCs device and to further understand the electron recombination in DSSCs. The EIS spectra were carried out under AM 1.5 G simulated solar light (100 mW cm^{-2}) at open circuit voltage conditions.

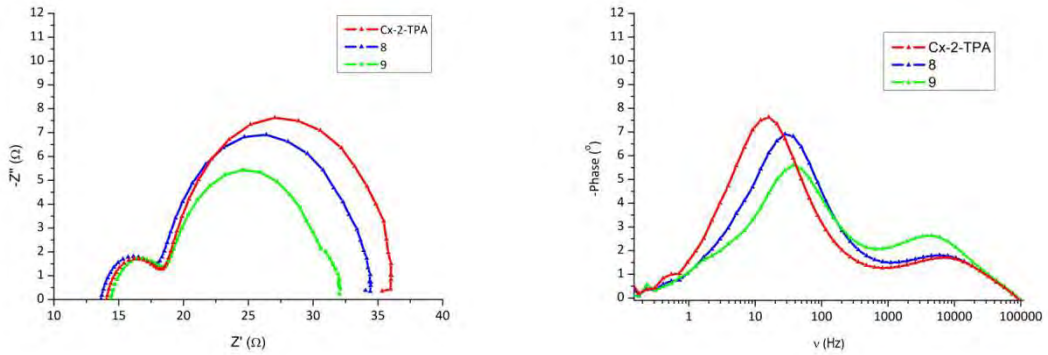

Fig 7. Nyquist (left) and Bode (right) plot of devices 6 µm, 5 h immersion time) prepared with dyes **Cx-2-TPA**, **8** and **9**

The Nyquist and Bode plots of the devices prepared with **Cx-2-TPA**, **8** and **9** are shown in **Fig. 7** and S.39. Two clear semicircles were observed in these Nyquist plots. The first semicircle, which is located in the high frequency region, is assigned to the charge transfer at the interface of counter electrode Pt and electrolyte (R_{ce}). The radius of the intermediate frequency semicircle in the Nyquist plot reflects electron transport resistance, and a smaller radius means a lower electron transport resistance. [43] According to these Figures, the electron transport resistance decreases from **8** to **9** [44] supporting that the BTZ is an adequate auxiliary electron withdrawing unit useful for improving the overall efficiency when applied to D-A- π -A organic sensitizers. Bode phase plots (**Fig.7** and S.39 (right)) were used to estimate the lifetime of electrons (τ) in the conduction band of TiO_2 [45,46]. The τ values are calculated using the equation $\tau = 1/(2\pi f)$ where f stands for the frequency at the maximum of the curve in the intermediate frequency region in the Bode plot. The order of τ values is **Cx-2-TPA** > **9** > **8**. These results suggest a more efficient hindering of the recombination processes on the TiO2 surface in the devices based on **Cx-2-TPA** and agree with their higher V_{oc} values as compared with **8** and **9-** based DSSCs. (See **Table 4** and **5**).

In order to study the stability of the device performance, the photovoltaic parameters have been measured over time. The results gathered in **Fig. 8** (devices 6 µm, 5 h immersion time) and **Fig. S. 40** (devices 13 µm, 24 h immersion time). The open circuit voltage and overall efficiency of these devices remains between 98 and 100 % of their initial values, essentially stable up to 500 h after the cell assembly.

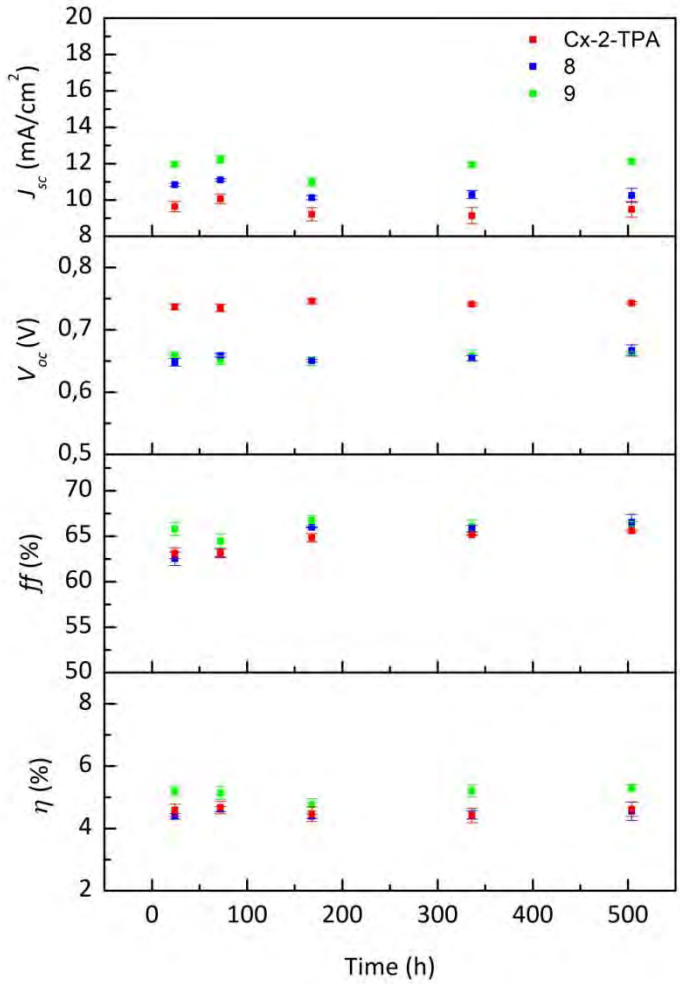

Fig 8. Detailed photovoltaic parameters of devices prepared with 6 μm thick electrodes and 5 h immersion time of dyes **Cx-2-TPA**, **8** and **9** measured under the irradiance of AM 1.5 G sunlight during successive full-sun visible-light soaking (1 sun 1000 W/m^2).

3. Conclusions

Novel multichromophoric calix[4]arenes have been prepared and their optical, electronic and photovoltaic properties have been evaluated and compared to previously described calix[4]arene derivative difunctionalized with TPA dye.

These dyes have both broader spectra and higher molar extinction coefficients than calix[4]arene difunctionalized with TPA dye, indicating that they have promising ability of light-capturing comparing with other triphenylamine-dyes.

The devices prepared with the benzothiadiazole-phenyl derivative show a broader IPCE spectrum than the ones prepared with the thiophene dye.

The use of thicker electrodes results in higher photocurrent density values and, although the open circuit voltage values are reduced, the overall efficiency of the devices is improved.

The calix[4]arene derivative based on phenylbenzothiadiazole has reached a value of 5.84 % which means an increase of 33 % over calix[4]arene difunctionalized TPA dye.

4. Experimental

4'-(((*tert*-butyldimethylsilyl)oxy)methyl)-5'-(4-(diphenylamino)phenyl)-[2,2'-bithiophene]-5-carbaldehyde 2

To a solution of compound **1** (400 mg, 0.85 mmol) in anhydrous THF (30 mL) at temperature of -78 ºC under argon atmosphere, a solution of *n*-butyllithium (1.6 M in THF) (0.68 mL (1.08 mmol) was slowly added. It was stirred at -50 °C for 1 hour. Then a solution of tributyltin chloride (0.28 mL, 0.96 mmol) was added and stirred for 5 minutes. Then, the reaction mixture was stirred at room temperature during 2 hours.

The reaction was quenched by the addition of 30 mL of diethyl ether and the organic layer was washed with brine and dried over magnesium sulfate. After concentration under reduced pressure, the yellow residue was used without purification in the next step.

In a flask with the yellow residue dissolved in 8 mL of toluene, a solution of 5-bromothiophene-2-carboxaldehyde (0.01 mL, 0.8 mmol) was added. The mixture was degassed with argon during 15 minutes. Then $Pd(PPh_3)_4$ (56 mg, 0.03 mmol) was added and the mixture was heated to 100 °C of temperature for 15 hours under argon atmosphere. The reaction was quenched by the addition of 40 mL of H_2O. The mixture was extracted with toluene (2 x 60 mL). The organic layer was washed with NH_4Cl (1 x 60 mL) and H_2O (2x60 mL), was dried over magnesium sulfate and the solvent was evaporated by reduced pressure. The residue was purified by flash chromatography (hexane/dichloromethane 1:1) and the aldehyde **2** was isolated as orange solid (293 mg, 63 %).

Molecular weight (g/mol): 581.86. **IR** (KBr, cm^{-1}) 1665 (C=O), 1595 (C=C). **^{1}H-NMR** (300 MHz, 298 K, CD_2Cl_2) δ (ppm): 0.12 (s, 6H), 0.95 (s, 9H), 4.73 (s, 2H), 7.09-7.18 (m, 9H), 7.30-7.36 (m, 4H), 7.39-7.42 (m, 2H), 7.46 (s, 1H), 7.72 (d, *J*=7.7 Hz, 1H), 9.88 (s, 1H). **^{13}C-NMR** (75 MHz, 298 K, CD_2Cl_2) δ (ppm): -4.9, 26.3, 30.4, 60.0, 123.3, 124.2, 124.6, 125.6, 127.2, 129.4, 130.0, 130.3, 133.8, 138.1, 139.2, 142.2, 142.4, 147.6, 148.0, 148.7, 183.0. **HRMS** (ESI^+) m/z: calculated for $[C_{34}H_{35}O_2NS_2Si]^+$ 581.1873. Found: 581.1880 $[M]^{+\cdot}$.

4-(7-(4-(((*tert*-butyldimethylsilyl)oxy)methyl)-5-(4-(diphenylamino)phenyl)thiophen-2-yl)benzo[c][1,2,5]thiadiazol-4-yl)benzaldehyde 3

To a solution of compound **1** (337 g, 0.72 mmol) in anhydrous THF (25 mL) at temperature of -78 ºC under argon atmosphere, a solution of *n*-butyllithium (1.6 M in THF) (0.58 mL, 0.93 mmol) was slowly added. It was stirred at -50 °C for 1 hour. Then a solution of tributyltin chloride (0.24 mL, 0.86 mmol) was added and stirred for 5 minutes. After that, the reaction mixture was stirred at room temperature during 2 hours.

The mixture of reaction was quenched by the addition of 25 mL of diethyl ether and the organic layer was washed with brine and dried over magnesium sulfate. After concentration under reduced pressure, the yellow residue was used without purification in the next step.

In a flask with the yellow residue dissolved in 8 mL of toluene, a solution of 4-(7-bromobenzo[*c*][1,2,5]tiadiazol-4-yl)-benzaldehyde (230 mg, 0.72 mmol) was added. The mixture was degassed with argon during 15 minutes. Then $Pd(PPh_3)_4$ (47 mg, 0.025 mmol) was

added and the mixture was heated to 100 °C of temperature for 15 hours under argon atmosphere. The reaction was quenched by the addition of 30 mL of H_2O. The mixture was extracted with toluene (2x60 mL). The organic layer was washed with NH_4Cl (1x60 mL) and H_2O (2x60 mL), was dried over magnesium sulfate and the solvent was evaporated by reduced pressure.

The residue was purified by flash chromatography (hexane/dichloromethane 1:1) and the aldehyde **3** was isolated as a red solid (342 mg, 67 %).

Molecular weight (g/mol): 709.99. **Melting point (°C) at 760 mm Hg**: 85-87. **IR** (KBr, cm^{-1}) 1694 (C=O), 1583 (C=C) **^{1}H-NMR** (300 MHz, 298 K, $CDCl_3$) δ (ppm): 0.15 (s, 6H), 0.95 (s, 9H), 4.81 (s, 2H), 7.04-7.19 (m, 8H), 7.27-7.34 (m, 4H), 7.45 (d, *J*=8.7 Hz, 2H), 7.81 (d, *J*=7.5 Hz, 1H), 7.95 (d, *J*=7.5 Hz, 1H), 8.05 (d, *J*=8.4 Hz, 2H), 8.17 (d, *J*=8.4 Hz, 2H), 8.25 (s, 1H), 10.11 (bs, 1H). **^{13}C-NMR** (75 MHz, 298 K, $CDCl_3$) δ (ppm): -4.9, 26.1, 29.8, 59.9, 123.1, 123.5, 124.9, 127.8, 129.1, 129.5, 129.8, 130.1, 130.9, 131.1, 135.9, 136.4, 138.3, 142.4, 143.4, 147.6, 147.9, 153.8, 192.2. **HRMS** (ESI^+) m/z : Calculated for $[C_{42}H_{39}O_2N_3NaS_2Si]^+$: 732.2145. Found: 732.2152 $[M+Na]^+$.

5'-(4-(diphenylamino)phenyl)-4'-(hydroxymethyl)-[2,2'-bithiophene]-5-carbaldehyde 4

To a solution of compound **2** (300 mg, 0.51 mmol) in THF (15 mL) at temperature of 0° C under Argon, a solution of tetrabutylammonium fluoride (1 M THF) (1.02 mL, 1.02 mmol) was slowly added and was stirred for 2 hours. The resulting solution was quenched by the addition of 50 mL of NH_4Cl saturated solution (aq). The aqueous phase was extracted with ethyl acetate solution and the organic phase was dried over dry $MgSO_4$ and the solvent was evaporated by reduced pressure. The residue was purified by flash chromatography using hexane/ethyl acetate from (6:4) to yield a yellow solid (195 mg, 82 %).

Molecular weight (g/mol): 467.60. **Melting point (°C) at 760 mm Hg**: 174-176. **IR** (KBr, cm^{-1}): 3429 (O-H), 1630 (C=O), 1583 (C=C). **^{1}H-NMR** (300 MHz, 298 K, CD_2Cl_2) δ (ppm): 4.67 (s, 2H), 5.33(s, 1H), 7.04-7.16 (m, 8H), 7.34-7.26 (m, 5H), 7.38 (d, *J*= 8.7 Hz, 2H), 7.46 (s, 1H), 7.69 (d, *J*= 3.9 Hz, 1H), 9.81 (s, 1H). **^{13}C-NMR** (75 MHz, 298 K, CD_2Cl_2) δ (ppm): 58.7, 122.5, 123.6, 124.0, 125.0, 126.1, 128.5, 129.4, 129.6, 133.5, 137.5, 138.0, 141.6, 142.7, 146.7, 147.2, 148.2, 182.4 **HRMS** (ESI^+): Calculated for $[C_{28}H_{22}O_2NS_2]^+$: 468.1086. Found: 468.1061 $[M+H]^+$.

4-(7-(5-(4-(diphenylamino)phenyl)-4-(hydroxymethyl)thiophene-2-yl)benzo[c][1,2,5]thiadiazol-4-yl)benzaldehyde 5

To a solution of compound **3** (325 mg, 0.46 mmol) in dry THF (15 mL) at temperature of 0°C under Argon, a solution of tetrabutylammonium fluoride (1 M THF) (0.96 mL, 0.96 mmol) was slowly added and was stirred for 2 hours. The resulting solution was quenched by the addition of 50 mL of NH_4Cl saturated solution (aq). The aqueous phase was extracted with ethyl acetate solution and the organic phase was dried over dry $MgSO_4$ and the solvent was evaporated by reduced pressure. The residue was purified by flash chromatography using hexane/ethyl acetate from (6:4) to yield a red solid (158 mg, 58 %).

Molecular weight (g/mol): 595.73. **Melting point (°C) at 760 mm Hg :** 203-205. **IR** (KBr, cm^{-1}): 3448 (O-H), 1670 (C=O), 1583 (C=C). **^{1}H-NMR** (300 MHz, 298 K, CD_2Cl_2) δ (ppm): 4.75 (s, 2H), 7.04-7.20 (m, 8H), 7.26-7.35 (m, 4H), 7.47 (d, *J*=8.7 Hz, 2H), 7.79 (d, *J*=7.8 Hz, 1H), 7.94 (d, *J*=7.8 Hz, 1H), 8.00 (d, *J*=8.3 Hz, 2H), 8.15 (d, *J*=8.3 Hz, 2H), 8.24 (s, 1H), 10.07 (s, 1H). **^{13}C-NMR** (75 MHz, 298 K, CD_2Cl_2) δ (ppm): 59.4, 123.3, 124.0, 125.4, 127.3, 127.6, 129.4, 129.9, 130.2,

131.2, 131.3, 136.3, 137.1, 138.3, 143.4, 143.5, 147.9, 148.5, 154.2, 192.3. **HRMS** (ESI^+): Calculated for $[C_{36}H_{25}O_2N_3NaS_2]^+$: 618.1280. Found: 618.1296 $[M+Na]^+$.

Calix[4]arene derivative of (4) compound 6

To a solution of calixarene diacid **Cx-2** (110 mg, 0.12 mmol), 4-dimethylaminopyridine (DMAP) (13 mg, 0.109 mmol) and 1-ethyl-3-[3-dimethylaminopropyl]carbodiimide hydrochloride (EDC) (134.2 mg, 0.68 mmol) were successively added. This mixture was maintained at temperature of 0 °C during 30 min. Alcohol **4** (130 mg, 0.24 mmol) was added. The reaction mixture was then stirred at room temperature for 3 days. Then it was washed and dried over magnesium sulfate and the solvent was evaporated by reduced pressure. The residue was purified by flash chromatography using hexane/ethyl acetate from (8:2) to yield a yellow solid (130 mg, 59 %).

Molecular weight (g/mol): 1832.48. **Melting point (°C) at 760 mm Hg**: 109-111. **IR** (KBr, cm^{-1}) 1740 (C=O), 1664 (C=O) **^{1}H-NMR** (300 MHz, 298 K, CD_2Cl_2) δ (ppm): 0.97 (t, *J*=7.5 Hz, 6H), 1.09 (s, 18H), 1.11 (s, 18H), 1.77-1.87 (m, 4H), 1.96-2.08 (m, 8H), 2.49 (t, *J*=7.5 Hz, 4H), 3.10 (d, *J*=12.6 Hz, 4H), 3.78 (t, *J*= 7.5 Hz, 4H), 3.87 (t, *J*=7.5 Hz, 4H), 4.38 (d, *J*=12.6 Hz, 4H), 5.11 (s, 4H), 6.80 (s, 4H), 6.81 (s, 4H), 7.07-7.16 (m, 16H), 7.26 (d, *J*=4.0 Hz, 2H), 7.28-7.37 (m, 12H), 7.43 (s, 2H), 7.68 (d, *J*=4.0 Hz, 2H), 9.85 (s, 2H). **^{13}C-NMR** (75 MHz, 298 K, CD_2Cl_2) δ (ppm): 10.7, 22.2, 23.9, 30.2, 31.5, 31.7, 31.7, 34.2, 34.7, 60.3, 75.2, 77.5, 122.8, 124.2, 124.7, 125.5, 125.6, 126.1, 129.4, 129.9, 130.2, 133.3, 134.1, 134.3, 134,3, 137.8, 142.3, 144.7, 144.8, 145.0, 146.9, 147.7, 148,9, 154.0, 154.2, 173.5, 182.8. **MS** ($MALDI^+$) *m/z*: 1831 $[M]^{+\cdot}$.

Calix[4]arene derivative of (5) compound 7

To a solution of calixarene diacid **Cx-2** (110 mg, 0.13 mmol), 4-dimethylaminopyridine (DMAP) (13 mg, 0.109 mmol)) and 1-ethyl-3-[3-dimethylaminopropyl]carbodiimide hydrochloride (EDC) (160.8 mg, 0.81 mmol) were successively added. This mixture was maintained at 0°C during 30 min. Alcohol **5** (150 mg, 0.26 mmol) was added. The reaction mixture was then stirred at room temperature for 5 days. The organic layer was washed and dried over magnesium sulfate and the solvent was evaporated by reduced pressure. The residue was purified by flash chromatography using hexane/ethyl acetate from (8:2) to yield a yellow solid (150 mg, 55 %).

Molecular weight (g/mol): 2088.7. **Melting point (°C) at 760 mm Hg:** 124-126. **IR** (KBr, cm^{-1}) 1741 (C=O), 1691 (C=O) **^{1}H-NMR:** (300 MHz, 298 K, CD_2Cl_2) δ (ppm): 0.93 (t, *J*=7.5 Hz, 6H), 1.03 (s, 18H), 1.10 (s, 18H), 1.74-1.86 (m, 4H), 1.90-1.98 (m, 4H), 2.04-2.10 (m, 4H), 2.50 (t, *J*=7.8 Hz, 4H), 3.07 (d, *J*=12.6 Hz, 4H), 3.71 (t, *J*= 7.6 Hz, 4H), 3.88 (t, *J*=7.7 Hz, 4H), 4.34 (d, *J*=12.6 Hz, 4H), 5.16 (s, 4H), 6.72 (s, 4H), 6,82 (s, 4H), 7.04-7.15 (m, 16H), 7.25-7.32 (m, 8H), 7.36-7.42 (m, 4H), 7.72 (d, *J*=7.5 Hz, 2H), 7.85 (d, *J*=7.5 Hz, 2H), 7.97 (d, *J*=8.4 Hz, 4H), 8.11 (d, *J*=8.4 Hz, 4H), 8.15 (s, 2H), 10.06 (s, 2H). **^{13}C-NMR** (75 MHz, 298 K, CD_2Cl_2) δ (ppm): 10.6, 22.1, 23.8, 30.2, 31.3, 31.6, 31.6, 34.1, 34.1, 34.7, 60.5, 75.1, 77.4, 122.9, 124.0, 125.2, 125.3, 125.4, 125.5, 126.6, 127.2, 129.2, 130.1, 132.8, 134.5, 136.2, 137.7, 143.3, 144.6, 147.7, 148.6, 152.8, 153.9, 154.0, 154.1, 173.5, 192.0. **MS** ($MALDI^+$) *m/z*: 2087 $[M]^{+\cdot}$.

Dye 8

To a solution of dialdehyde **6** (110 mg , 0.060 mmol) and 2-cyanoacetic acid (45 mg, 0.525 mmol) in chloroform (10 mL) piperidine (3.16 mL; 32 mmol) was added. The mixture was heated at temperature of 65 ° C for 5 days under argon atmosphere and prevented for light, then it was cooled down to room temperature. After concentration under reduced pressure, the resulting solid was dissolved with CH_2Cl_2, acidified with HCl 0.1 M, and was washed with

water. The solution was dried and the solvent was removed under reduced pressure. The resulting solid was washed with cold MeOH and a black solid was obtained (45 mg, 38 %).

Molecular weight (g/mol): 1966.6. **Melting point (°C) at 760 mm Hg**: 173-175. **IR** (KBr, cm^{-1}) 3438 (O-H), 2222 (C≡N), 1732 (C=O), 1584 (C=C). **^{1}H-NMR:** (500 MHz, 353 K, DMF- d_7) δ (ppm): 0.97 (t, *J*= 7.4 Hz, 6H), 1.11 (s, 18H), 1.12 (s, 18H), 1.78-1.88 (m, 4H), 1.90-2.02 (m, 4H), 2.04-2.12 (m, 4H), 2.47-2.55 (m, 4H), 3.15 (d, *J*= 12.4 Hz, 4H), 3.76-3.84 (m, 4H), 3.83-3.91 (m, 4H), 4.39 (d, *J*= 12.4 Hz, 4H), 5.16 (s, 4H), 6.80-6.95 (m, 8H), 7.03-7.21(m, 16H), 7.28-7.53 (m, 16H), 7.55-7.70 (m, 2H), 7.80-7.90 (m, 2H), 8.35-8.50 (m, 2H). **MS** (MALDI$^+$) *m/z*: 1988 $[M+Na]^+$.

Dye 9

To a solution of dialdehyde **7** (150 mg, 0.072 mmol) and 2-cyanoacetic acid (45mg, 0.525 mmol) in chloroform (10 mL) piperidine (2.35 mL; 23.7 mmol) was added. The mixture was heated at temperature of 65° C for 5 days under argon atmosphere and prevented for light, then it was cooled down to room temperature. It was acidified with HCl 0.1 M, and was washed with water. The solution was dried and the solvent was removed under reduced pressure. The resulting solid was dissolved with CH_2Cl_2 and cold MeOH was added, then a black solid was obtained (95 mg, 59 %).

Molecular weight (g/mol): 2222.8. **Melting point (°C) at 760 mm Hg**: 195-197. **IR** (KBr, cm^{-1}) 3430 (O-H), 2214 (C≡N), 1733 (C=O), 1592 (C=C). **^{1}H-NMR:** (500 MHz, 353 K, DMF- d_7) δ (ppm): 0.96 (bt, 6H), 1.03 (bs, 18H), 1.16 (bs, 18H), 1.80-1.88 (m, 4H), 1.89-1.99 (m, 4H), 2.02-2.19 (m, 4H), 2.61 (bt, 4H), 3.14 (m, 4H), 3.71 (bt, 4H), 3.90 (bt, 4H), 4.38 (m, 4H), 5.21 (bs, 4H), 6.79 (bs, 4H), 6.95 (bs, 4H), 7.06-7.19 (m, 16H), 7.34-7.40 (m, 8H), 7.46-7.54 (m, 4H), 7.95-8.02 (m, 4H), 8.05-8.10 (m, 4H), 8.12-8.21 (m, 4H), 8.22-8.30 (m, 4H), 8.32-8.50 (m, 2H). **MS** (MALDI$^+$) m/z: 2221 $[M]^{+\cdot}$.

Acknowledgements

We gratefully acknowledge the financial support from the Spanish Ministry of Science and Innovation-MICINN-FEDER (Project CTQ2014–52331-R) and Gobierno de Aragón-Fondo Social Europeo (E14_17R). The "ICMA-Pi2 program" is gratefully acknowledged for the fellowship (EC). ID and DB acknowledge for the financial support of DGA fellowship and PhD studentship Santander-2018 programs, respectively. Moreover, anonymous referees are gratefully acknowledged for helpful suggestions.

References

[1] O'Regan B, Grätzel M. A low-cost, high-efficiency solar cell based on dye-sensitized colloidal TiO_2 films. Nature 1991; 353:737-40. http://dx.doi.org/10.1038/353737a0

[2] Zhang XY, Gratzel M, Hua JL. Donor design and modification strategies of metal-free sensitizers for highly-efficient n-type dye-sensitized solar cells. Frontiers of optoelectronics, 2016; 9:3-37. http://dx.doi.org/10.1007/s12200-016-0563-x

[3] Lin R Y-Y, Wu FL, Chang CH, Chou H-H, Chuang T-M, Chu T-C, Hsu C-Y, Chen P-W, Ho K-C, Lo Y-H, Lin J-T. Y-shaped metal-free D–π–$(A)_2$ sensitizers for high-performance dye-sensitized solar cells. J Mater Chem A, 2014; 2: 3092-3101. http://dx.doi.org/10.1039/C3TA14404F

[4] Zang X-F, Zhang T-L, Huang Z-S, Iqbal Z, Kuang D-B, Wang L, Meier H, Cao D. Impact of the position isomer of the linkage in the double D-A branch-based organic dyes on the photovoltaic performance. Dyes Pigm 2014;104:89-96. https://doi.org/10.1016/j.dyepig.2013.12.028

[5] Mishra A, Ficher MKR, Bauerle P. Metal-free organic dyes for dye-sensitized solar cells: From structure: property relationships to design rules. Angew Chem, Int Ed 2009;4:2474-99. http://dx.doi.org/10.1002/anie.200804709

[6] Ning Z, Fu Y, Tian H. Improvement of dye-sensitized solar cells: what we know and what we need to know. Energy Environ Sci 2010;3:1170-81. http://dx.doi.org/10.1039/C003841E

[7] Wan, ZQ, Jia, C Y, Wang Y, Yao XY. Dithiafulvenyl–triphenylamine organic dyes with alkyl chains for efficient coadsorbent-free dye-sensitized solar cells. RSC Adv 2015;5:50813-20. http://dx.doi.org/10.1039/C5RA06774J

[8] Tang J, Hua J, Wu W, Li J, Jin Z, Long Y, Tian H. New starburst sensitizer with carbazole antennas for efficient and stable dye-sensitized solar cells Energy Environ Sci 2010;3:1736-53. http://dx.doi.org/10.1039/C0EE00008F.

[9] Ning Z, Zhang Q, Pei H, Luan J, Lu C, Cui Y, Tian H. Photovoltage Improvement for Dye-Sensitized Solar Cells via Cone-Shaped Structural Design. J. Phys. Chem. C, 2009;113:10307-13. http://dx.doi.org/10.1021/jp902408z

[10] Joly D, Godfroy M, Pellejà L, Kervella Y, Maldivi P, Narbey S, Oswald F, Palomares E, Demadrille R. Side chain engineering of organic sensitizers for dye-sensitized solar cells: a strategy to improve performances and stability. J Mater Chem A, 2017, 5, 6122-30. http://dx.doi.org/10.1039/c7ta00793k

[11] Zhang L, Cole JM. Dye aggregation in dye-sensitized solar cells. Mater Chem A, 2017, 5, 19541-59. http://dx.doi.org/10.1039/C7TA05632J

[12] Hampton PD, Bencze Z, Tong WD, Daitch C. A new synthesis of oxacalix[3]arene macrocycles and alkali metal binding studies. J Org Chem 1994;59:4838-43 http://dx.doi.org/10.1021/jo00096a026

[13] See KA, Fronczek FR, Watson VW, Kashyap RP, Gutsche CD. Calixarenes. 26. Selective esterification and selective ester cleavage of calix[4larenes. J Org Chem 1991;56:7256-68. http://dx.doi.org/10.1021/jo00026a015

[14] Andreu R, Franco S, Garín J, Romero J, Villacampa B, Blesa MJ, Orduna J. Multichromophoric calix[4]arenes: Effect of interchromophore distances on linear and nonlinear optical properties. ChemPhysChem 2012;13:3204-9. http://dx.doi.org/10.1002/cphc.201200203

[15] Castillo-Vallés M, Andrés-Castán JM, Garín J, Orduna J, Villacampa B, Franco S, Blesa MJ. Dye-sensitized-solar-cells based on calix[4]arene scaffolds. RSC Adv 2015;5:90667-70. http://dx.doi.org/10.1039/c5ra15184h.

[16] Colom E, Andrés JM, Franco S, Garín J, Montoya J F, Orduna J, Villacampa B, Blesa MJ. Multichromophoric sensitizers based on calix[4]arene scaffold and *4H*-pyranylidene moiety for DSSCs application. Dyes Pigm 2017; 136: 505-14. http://dx.doi.org/10.1016/j.dyepig.2016.08.067

[17] Iwamoto K, Shinkai S. Syntheses and ion selectivity of all conformational isomers of tetra kis((ethoxycarbonyl)methoxy)calix[4]arene. J Org Chem 1992;57:7066-73. http://dx.doi.org/10.1021/jo00052a016

[18] Iwamoto K, Araki K, Shinkai S. Conformations and structures of tetra-0-alkyl-p-tert-butylcalix[4]arenes. How is the conformation of calix[4]arenes immobilized? J Org Chem 1991;56:4955-62. http://dx.doi.org/10.1021/jo00016a027

[19] Creaven BS, Donlona DF, McGinley J. Coordination chemistry of calix[4]arene derivatives with lower rim fuctionalization and their applications. Coord Chem Rev 2009;253:893-962. http://dx.doi.org/10.1016/j.ccr.2008.06.008

[20] Zhao BT, Blesa MJ, Mercier N, Le Derf F, Sallé M. Tetrathiafulvalene-appended Calix[4]arene: Synthesis and Electrochemical Characterization. Supramol Chem 2015;17:465-8. http://dx.doi.org/10.1080/10610270500211743

[21] Tan LL, Liu JM, Li SY, Xiao LM, Kuang DB, Su CY. Dye-sensitized solar cells with improved performance using cone-calix[4]arene based dyes. ChemSusChem 2015;8:280-7. http://dx.doi.org/10.1002/cssc.201402401

[22] Jia H, Ju X, Zhang M, Ju Z, Zheng H. Effects of heterocycles containing different atoms as pi-bridges on the performance of dye-sensitized solar cells. Phys Chem Chem Phys 2015;17:16334-40. http://dx.doi.org/10.1039/C5CP02 194D

[23] Joly D, Pellejà L, Narbey S, Oswald F, Meyer T, Kervella Y, Maldivi P, Clifford JN, Palomares E, Demadrille R. Metal-free organic sensitizers with narrow absorption in the visible for solar cells exceeding 10% efficiency. Energy Environ Sci 2015; 8, 2010. http://dx.doi.org/10.1039/c5ee00444f.

[24] Kim JJ, Choi H, Lee JW, Kang MS, Song K, Kang SO, Ko J. Polymer gel electrolyte to achieve ≥6 % power conversion efficiency with a novel organic dye incorporating a low-band- gap chromophore. J Mat Chem 2008;18:5223–9. http://dx.doi.org/10.1039/B809376H

[25] Haid S, Marszalek M, Mishra A, Wielopolski M, Teuscher J, Moser J E, Humphry-Baker R, Zakeeruddin SM, Grätzel M, Bäuerle P. Significant improvement of dye-sensitized solar cell performance by small structural modification in π-conjugated donor–acceptor dyes. Adv Funct Mater 2012;22: 1291–302. http://dx.doi.org/10.1002/adfm.201102519

[26] Liang M, Chen J. Arylamine organic dyes for dye-sensitized solar cells. Chem Soc Rev 2013;42:3453-88. http://dx.doi.org/10.1039/c3cs35372a

[27] Pérez-Tejada R, Martínez de Baroja N, Franco S, Pelleja L, Orduna J, Andreu R, Garín J. Organic sensitizers bearing a trialkylsilyl ether group for liquid dye sensitized solar cells. Dyes Pigm 2015; 123:293-303. http://dx.doi.org/10.1016/j.dyepig.2015.07.026

[28] Khadem M, Zhao Y. Tetrathiafulvalene Vinylogue−Fluorene Co-oligomers: Synthesis, Properties, and Supramolecular Interactions with Carbon Nanotubes. J Org Chem 2015; 80: 7419−29. http://dx.doi.org/ 10.1021/acs.joc.5b00792

[29] Sandanayaka ASD, Taguri Y, Araki Y, Ishi-i T, Mataka S, Ito O. Photoinduced Charge Separation and Charge Recombination in the [60]Fullerene-Diphenylbenzothiadiazole-Triphenylamine Triad: Role of Diphenylbenzothiadiazole as Bridge. J Phys Chem B 2005; 109: 22502-12. http://dx.doi.org/ 10.1021/jp053809c

[30] Leliege A, Le Regent C-H, Allain M, Blanchard P, Roncali J. Structural modulation of internal charge transfer in small molecular donors for organic solar cells. Chem. Commun 2012; 48: 8907-9. http://dx.doi.org/10.1039/C2CC33921H

[31] Blesa MJ, Zhao B, Allain M, Le Derf F, Sallé M. Bis(calixcrown)tetrathiafulvalene receptors. Chem Eur J 2006; 12: 1906–14. http://dx.doi.org/10.1002/chem.200500878

[32] Rudzevich Y, Fischer K, Schmidt M, Böhmer V. Fourfold tetraurea calix[4]arenes—potential cores for the formation of self-assembled dendrimers. Org Biomol Chem 2005; 3: 3916–25. http://dx.doi.org/10.1039/B509948J.

[33] Bitter I, Grün A, Téth G, Balázs B, Horváth G, Töke L. Tetrahedron 1998; 54: 3857–70, http://dx.doi.org/10.1016/S0040-4020(98)00112-4.

[34] Lin R Y-Y, Lee C-P, Chen Y-C, Peng J-D, Chu T-C, Cou H-H, Yang H-M, Lin J T, Ho –C. Benzothiadiazole-containing donor-acceptor-acceptor type organic sensitizers for solar cells with ZnO photoanodes. Chem Commun 2012; 48: 12071-3. http://dx.doi.org/10.1039/C2CC37184G

[35] Liu Z, Duan K, Guo H, Deng Y, Huang H, Yi X, Chen H, Tan S. The enhancement of photovoltaic properties of the DSSCs based on D-A-π-A organic dyes via tuning auxiliary acceptor. Dyes Pigm 2017; 140: 312-9. http://dx.doi.org/10.1016/j.dyepig.2017.01.026.

[36] Fuse S, Sugiyama S, Maitani MM, Wada Y, Ogomi Y, Hayase S, Katoh R, Kaiho T, Takahashi T. Elucidating the Structure–Property Relationships of Donor–π-Acceptor Dyes for Dye-Sensitized Solar Cells (DSSCs) through Rapid Library Synthesis by a One-Pot Procedure. Chem Eur J 2014; 20: 10685-94. http://dx.doi.org/10.1002/chem.201402093.

[37] Nüesch F, Grätzel M. H-aggregation and correlated absorption and emission of a merocyanine dye in solution, at the surface and in the solid state. A link between crystal structure and photophysical properties. Chem Phys 1995; 193: 1–17. http://dx.doi.org/10.1016/0301-0104(94)00405-Y.

[38] Hagfeldt A, Grätzel M. Light-Induced Redox Reactions in Nanocrystalline Systems. Chem Rev 1995; 95 (1), 49–68. http://dx.doi.org/10.1021/cr00033a003

[39] Pazoki M, Cappel U B, Johansson E M J, Hagfeldt A, Boschloo G. Characterization techniques for dye-sensitized solar cells. Energy Environ Sci, 2017; 10, 672-709. http://dx.doi.org/10.1039/c6ee02732f

[40] Wu Y,' Zhu W. Organic sensitizers from D–π–A to D–A–π–A: effect of the internal electron-withdrawing units on molecular absorption, energy levels and photovoltaic performances. Chem Soc Rev 2013; 42**,** 2039-58. http://dx.doi.org/10.1039/C2CS35346F.

[41] Zhou G, Pscirer N, Schoneboom JC, Eickemeyer F, Baumgarten M, Mullen K. Ladder-type pentaphenylene dyes for dye-sensitized solar cells. Chem Mater 2008; 20: 1808-15. http://dx.doi.org/10.1021/cm703459p.

[42] Roh A D-H, Kim K M, Nam J S, Kim, U-Y, Kim B-M, Kim J S, Kwon T-H. Strategy for Improved Photoconversion Efficiency in Thin Photoelectrode Films by Controlling π-Spacer Dihedral. J Phys Chem C 2016; 120, 24655−66. http://dx.doi.org/10.1021/acs.jpcc.6b0826.

[43] Chen Y-C, Chen Y-H, Chou H-H, Chaurasia S, Wen YS, Lin JT and Yao C-F. Naphthyl and Thienyl Units as Bridges for Metal-Free Dye-Sensitized Solar Cells. Chem Asian J 2012; 7, 1074 – 84. http://dx.doi.org/10.1002/asia.201100972

[44] Lin RY-Y, Wu F-L, Chang C-H, Chou H-H, Chuang T-M, Chu T-C, Hsu C-Y, Chen P-W, Ho K-C, Lo Y-H, Lin J-T. Y-shaped metal-free D–p–$(A)_2$ sensitizers for high-performance dye-sensitized solar cells. J Mater Chem A, 2014; 2: 3092–101. http://dx.doi.org/10.1039/c3ta14404f.

[45] Kern R, Sastrawan R, Ferber J, Stangl R, Luther J. Modeling and interpretation of electrical impedance spectra of dye solar cells operated under open-circuit conditions. ElectrochimActa 2002;47:4213–25. https://doi.org/10.1016/S0013-4686(02)00444-9

[46] Wang Q, Moser J-E, Gratzel M. Electrochemical impedance spectroscopic. J. Phys. Chem. B, 2005, 109, 14945–53. http://dx.doi.org/110.1021/jp052768h

HIGHLIGHTS

The effectiveness of the use of *p-tert*-butylcalix[4]arene scaffold in avoiding aggregation has been confirmed.

The devices prepared with the new dyes showing red shifted and enhanced absorption spectra result in a better photovoltaic performance with respect to calix[4]arene derivatives bearing TPA dye

The inclusion of benzothiadiazole as an auxiliary electronwithdrawing unit improves the photocurrent density and the overall efficiency.